The University of Alabama
Department of Chemistry

Dye Sensitized Solar Cells

Literature Seminar

By

Haiying Wan

Tuesday, November 23, 2004

Introduction

Of the many problems facing mankind, those concerning the availability and distribution of energy will ultimately be the most important. As fossil fuel become depleted, we will turn more and more to alternative sources and eventually depend on energy technologies based on nuclear fusion, nuclear fission and solar energy. Nuclear energy also relies on finite resources and involves significant problems.

The sun's energy is the primary source for most energy forms found on the earth. Solar energy is clean, abundant, and renewable. Solar energy holds tremendous potential to benefit our world by diversifying our energy supply, reducing our dependence on imported fuels, improving the quality of the air we breathe, and stimulating our economy by creating jobs in the manufacture and installation of solar energy systems.

Currently, a significant and growing solar industry in the world is serving customers by providing solar water heating, pool heating, and solar-electric systems [1]. However, significant benefits to costumers will only be achieved when solar energy components are successfully integrated into homes, buildings, and power plants. To date, many of the solar energy systems are significantly more expensive than the traditional options available to customers (e.g., engines, gas heaters, grid electricity). The cost, performance, and convenience of these systems must be improved if solar energy is going to compete in energy markets against more traditional alternatives. Some large-scale solar technologies are close to being cost competitive, but the risk of making such a large investment is an obstacle to commercialization.

Background

The first panchromatic film, able to render the image of a scene realistically into black and white, followed the work of Vofel in Berlin after 1873 [2] in which he associated dyes with silver halide grains. The first sensitization of a photoelectrode was reported shortly, using the same chemistry [3]. However, the clear recognition of the parallelism between the two procedures, a realization that the same dyes in principle can function in both [4] and a verification that their operating mechanism is by injection of electrons from photo-excited dye molecules into the conduction band of the n-type semiconductor substrates [5] date from the 1960s. The dye sensitized solar cell (DYSC) has been around for a long time, but obtained only low conversion efficiencies, since a relatively thick layer of dye was used. Since the overall light absorption of a dye monolayer were low, limited the photocurrent efficiency with respect to the incident light to a value well below 1%. Semiconductors in mesoporous membrane type film with a high surface area led to an efficient light absorption by attached sensitizers and resulted in intensely colored photo anodes. After the announcement of surprisingly high efficiencies by O'Regan and Graẗzel in the early-1990s [6], this type of solar cell is under reinforced development aiming at large area and low cost solar cells [7].

Operation principle of the dye sensitized solar cell (DYSC)

The dye sensitized solar cell is composed of two surfaces of transparent conductor (mostly a conducting oxide on glass), onto one of which a few μm thick film of wide band gap semiconductor has been deposited in the form of a self-connected network of

nm-sized particles, with a net work of similarly or large sized self- connected pores in between the particles.

Energy conversion in a DYSC is based on the injection of an electron from a photoexcited state of the sensitizer dye (typically a bipyridine metal complex) into the conduction band of the nanocrystalline semiconductor (TiO_2 is by far the most employed oxide semiconductor), as depicted in Fig. 1 [8]. These cells also employ a liquid electrolyte (usually an iodide/triiodide redox-active couple dissolved in an or-ganic solvent) to reduce the dye cation (viz., regenerate the ground state of the dye). Regeneration of iodide ions, which are oxidized in this reaction to triiodide, is achieved at a platinized counter electrode, Eqs.(1)-(6):

$$TiO_2|S + h\nu \_ TiO_2|S^* \quad (1)$$

$$TiO_2|S^* \_ TiO_2|S^+ + e^- \quad (2)$$

$$TiO_2|S^+ + e^- \_ TiO_2|S \quad (3)$$

$$TiO_2|S^+ + 3/2I^- \_ TiO_2|S + 1/2\ I_3^-. \quad (4)$$

$$1/2\ I_3^- + e- \_ 3/2\ I^- \quad (5)$$

$$I_3^- + 2e- \rightarrow 3I^- \quad (6)$$

S: represents the dye sensitizer

Dye Molecules

An efficient photosensitizer should fulfill some requirements such as an intense absorption in the visible region, strong adsorption onto the semiconductor surface and efficient electron injection into the conduction band of the semiconductor. Moreover, it must be rapidly regenerated by the mediator layer in order to avoid electron recombination processes and be fairly stable, both in the ground and excited states. The

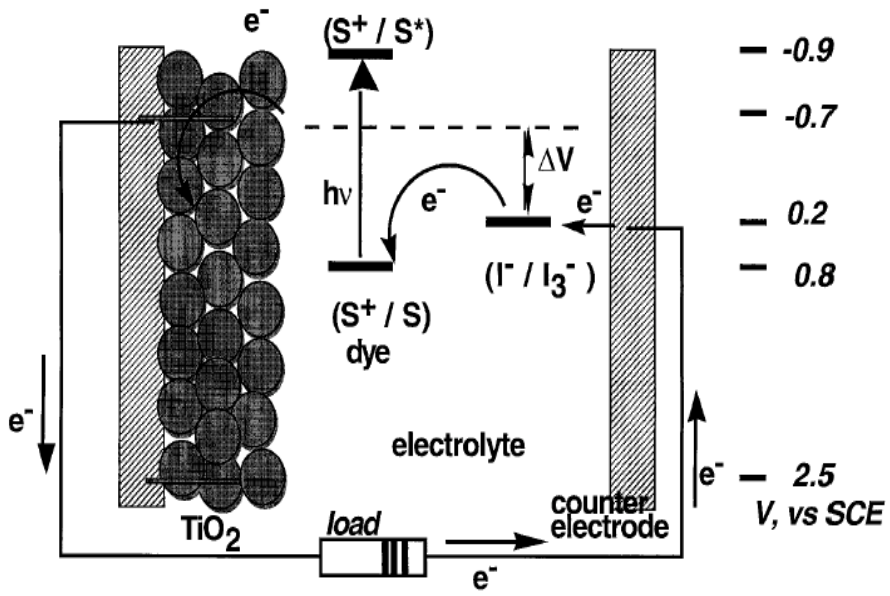

Figure 1. Principle of operation and energy level scheme of the dye-sensitized nanocrystalline solar cell (DYSC) photoexcitation of the sensitizer (S) is followed by electron injection into the conduction band of the mesoporous oxide semiconductor. The dye molecule is regenerated by the redox system, which itself is regenerated at the counter electrode by electrons passed through the load. Potentials are referred to the standard calomel electrode (SCE)

*Taken from the Fig. 1 of Ref. 8

ideal sensitizer photovoltaic cell converting standard global AM (air mass) 1.5 sunlight to electricity should absorb all light below a threshold wavelength of about 900 nm, which is equivalent to a semiconductor with a band gap of 1.4 eV. The best photovoltaic performance both in terms of conversion yield and long term stability has so far been achieved with polypyridyl complexes of ruthenium and osmium. Sensitizers having the general structure ML_2X_2 where L stands for 2,2'-bipyridyl-4,4'-dicarboxylic acid, $dcbH_2$,, M is Ru or Os and X presents a halide, cyanide, thiocyanate, [9,10] or water substituent, are particularly promising. Thus, the ruthenium complex cis-$RuL_2(NCS)_2$, known as N3 dye, has become the paradigm of heterogeneous charge transfer sensitizers for solar cells. The fully protonated N3 has absorption maxima at 518 and 380 nm, the extinction coefficients being 1.3 and 1.33 _10^4 M^{-1} cm^{-1}, respectively. The complex emits at 750 nm, the lifetime being 60 ns. The optical transition has MLCT (metal-to-ligand charge

transfer) character: excitation of the dye involves transfer of an electron from the metal to the π* orbital of the surface anchoring carboxylated bipyridyl ligand, from where it is released within less than 100 femto-second [11,12] into the conduction band of TiO_2, generating electric charges with unit quantum yield.

Since N3 was reported as a very efficient energy conversion dye, efforts have been made to either match or improve its performance. Recently a credible challenger have been identified, the 'black dye' (tri(cyanato)-2,2',2''-terpyridyl-4,4',4''-tricarboxylate)Ru(II) [13]. Figure 2 [8] compares the spectral response of the photocurrent observed with the two sensitizers. The incident photon to current conversion efficiency (IPCE) of the DYSC is plotted as a function of excitation wavelength. Both chromophores show high IPCE values in the visible range. However, the response of the black dye extends 100 nm further into the IR than that of N3. The photocurrent onset is close to 920 nm, i.e. near the optimal threshold for single junction converters. From there on the IPCE rises gradually (see Table 1 [14]), until at 700 nm it reaches a plateau of *ca* 80%. If one accounts for reflection and absorption losses in the conducting glass, the conversion of incident photons to electric currents is practically quantitative over the whole visible domain. From the overlap integral of the curves in Figure 2 with the AM1.5 solar radiation, one predicts the short circuit photocurrents of the N3 and black dye-sensitized cells to be 16 mA/cm^2 and 20.5 mA/cm^2, respectively, in agreement with experimental observations. The overall efficiency (η_{cell}) of the photovoltaic cell is calculated from the integral photocurrent density (i_{ph}), the open-circuit photovoltage (V_{oc}), the fill factor of the cell (*FF*) and the intensity of the incident light (*Is* =100 mW/cm^2)

$$\eta_{cell} = i_{ph} \times V_{oc} \times FF / I_s \qquad (7)$$

The performance in solar cells of N3 is shown in Table 1.

Table 1
Photoelectrochemical data obtained with solar cell sensitized by *cis*-[Ru(dcbH$_2$)$_2$(NCS)$_2$]

V_{oc} (V)	I_{sc} (mA cm^{-2})	IPCE$_{max}$ (%)	ff	η_{cell} (%)	Remarks
0.61	6.4		0.42	6.1	
0.640	5.0		0.76	10.4	a,b
0.660	7.9		0.76	10.4	a,c
0.670	11.5		0.74	10.3	a,d
0.720	18.2		0.73	10.0	a,e

[a] AM 1.5, light intensity.
[b] 24.1 mW cm^{-2}.
[c] 38.2 mW cm^{-2}.
[d] 55.6 mW cm^{-2}.
[e] 96.0 mW cm^{-2}.

*Taken from the part of Table 1 of Ref. 14

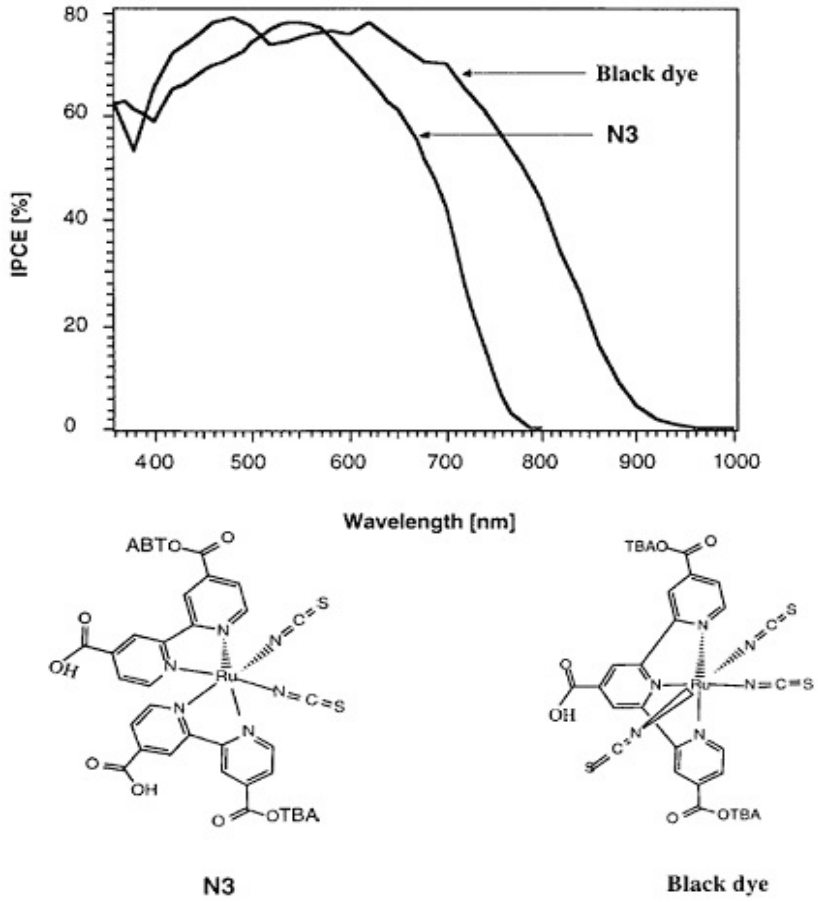

Figure 2 Spectral response curve of the photocurrent for the DYSC sensitized by N3 and the black dye. The incident photon to current conversion efficiency is plotted as a function of wavelength

*Taken from the Fig. 3 of Ref. 8

This search for efficient *cis*-[Ru(dcbH$_2$)2LL'] sensitizers has led to a wide variety of new photosensitizers [14]. Their spectroscopic properties are listed in Table 2 [14], while their performance in solar cells is shown in Table 3 [14]. Data presented in Table 3 point out that the substitution of the ancillary ligands has not, so far, improved the performance of the cells in terms of overall efficiency, _cell, or IPCE values, even though the new dyes could be successfully employed as semiconductor sensitizers. On the other hand, these new photosensitizers usually provide a wider coverage of the solar spectrum, promoting light harvesting in a lower energy region.

Table 2
Spectroscopic parameters of *cis*-[Ru(dcbH$_2$)$_2$LL'] evaluated as photosensitizers

Complex	Solvent	λ_{max} (nm) (ε_{max} (10^4 M^{-1} cm^{-1}))
[Ru(dcbH$_2$)$_2$(dmp)]Cl$_2$	EtOH	314 (1.68), 362 (sh), 514 (0.22)
[Ru(dcbH$_2$)$_2$(mdmp)]Cl$_2$	EtOH	246 (3.0), 316 (2.57), 364 (1.7), 550 (0.75)
[Ru(dcbH$_2$)$_2$(phdmp)]Cl$_2$	EtOH	314 (2.67), 366 (0.84), 410 (sh), 552 (0.33)
[Ru(dcbH$_2$)$_2$(blAlo)]Cl$_2$	EtOH	314 (1.55), 388 (0.615), 532 (0.52)
[Ru(dcbH$_2$)$_2$(pydmp)]Cl$_2$	EtOH	300 (0.34), 355 (0.22), 440 (0.75), 512 (0.56)
[Ru(dcbH$_2$)$_2$(aphb)]	DMF	350, 466
poly[Ru(dcbH$_2$)$_2$(aphb)	DMF	350, 476
Ru(dcbH$_2$)$_2$(qdt)	EtOH/MeOH	310 (2.58), 403 (0.94), 476 (0.86), 517 (0.88)
Ru(dcbH$_2$)$_2$(ecda)	EtOH/MeOH	313 (3.21), 402 (1.75), 500 (0.84), 582 (0.98)
Ru(dcbH$_2$)$_2$(bdt)	EtOH/MeOH	309 (3.23), 463 (0.95), 662 (0.21)
Ru(dcbH$_2$)$_2$(tdt)	EtOH/MeOH	307 (3.20), 470 (0.96), 670 (0.20)

Bibliography since 1998.

*Taken from the part of Table 2 of Ref. 14

Table 3
Photoelectrochemical data obtained with solar cell sensitized by *cis*-[Ru(dcbH$_2$)$_2$LL']

Complex	V_{oc} (V)	I_{sc} (mA cm^{-2})	IPCE$_{max}$ (%)	ff	η_{cell} (%)
[Ru(dcbH$_2$)$_2$(dmp)]Cl$_2$	0.289	0.315	33.24	0.55	2.0
[Ru(dcbH$_2$)$_2$(mdmp)]Cl$_2$	0.330	0.400	42.21	0.61	3.2
[Ru(dcbH$_2$)$_2$(phdmp)]Cl$_2$	0.420	0.604	63.74	0.38	3.8
[Ru(dcbH$_2$)$_2$(blAlo)]Cl$_2$	0.320	0.390	41.15	0.45	2.2
[Ru(dcbH$_2$)$_2$(pydmp)]Cl$_2$	0.212	0.220	48.36	0.65	2.5
[Ru(dcbH$_2$)$_2$(aphb)]	0.58	5.5		0.48	1.51
poly[Ru(dcbH$_2$)$_2$(aphb)]	0.34	2.1		0.48	0.33
Ru(dcbH$_2$)$_2$(qdt)	0.595	11.1	45	0.70	3.7
Ru(dcbH$_2$)$_2$(ecda)	0.580	5.4	30	0.65	2.0
Ru(dcbH$_2$)$_2$(bdt)	0.540	2.1	7	0.66	0.7
Ru(dcbH$_2$)$_2$(tdt)	0.504	1.1		0.70	0.4

Bibliography since 1998.

*Taken from the part of Table. 3 of Ref. 14

Nanocrystalline Semiconductor Film

Nanocrystalline electronic junctions compose of a network of mesoscopic oxide or chalcogenide particles, such as TiO_2, ZnO, Fe_2O_3, Nb_2O_5, WO_3, Ta_2O_5 or Cds and CdSe, which are interconnected to allow for electronic conduction to take place. Typically a paster (covered with paste) containing the nanocrystalline semiconductor particles is applied by screen printing or scraper on a conducting support usually a glass coated with a transparent conducting oxide layer. Subsequent sintering produces a mesoporous film whose porosity varies from about 20 to 80%. The pores form an interconnected network that is filled with an electrolyte or with a solid charge transfer material such as an amorphous organic hole transmitter. In this way an electronic junction of extremely large contact area is formed displaying very interesting and unique optoelectronic properties.

The oxide material of choice for many of these systems has been TiO_2 [15]. Its properties are intimately linked to the material content, chemical composition, structure and surface morphology. From the point of the material content and morphology, two crystalline forms of TiO_2 are important, anatase and rutile (the third form, brookite, is difficult to obtain). Anatase is the low temperature stable form and gives mesoscopic films that are transparent and colorless. Figure 3 [8] shows the scanning electron micrograph of a typical TiO_2 (anatase) film deposited by screen printing on a conducting glass sheet (R = 8-10 _/square) that serves as current collector. The film thickness is typically 5-20 μm and TiO_2 mass about 1-4 mg/cm^2. Analysis of the layer morphology shows the porosity to be about 50%, the average pore size being 15 nm. The prevailing structures of the anatase nanoparticles are square-bipyramidal, pseudo cubic. According

to high resolution Transmission Electron Microscopy (HRTEM) measurements, the (101) face is mostly exposed followed by 100 and 001 surface orientations.

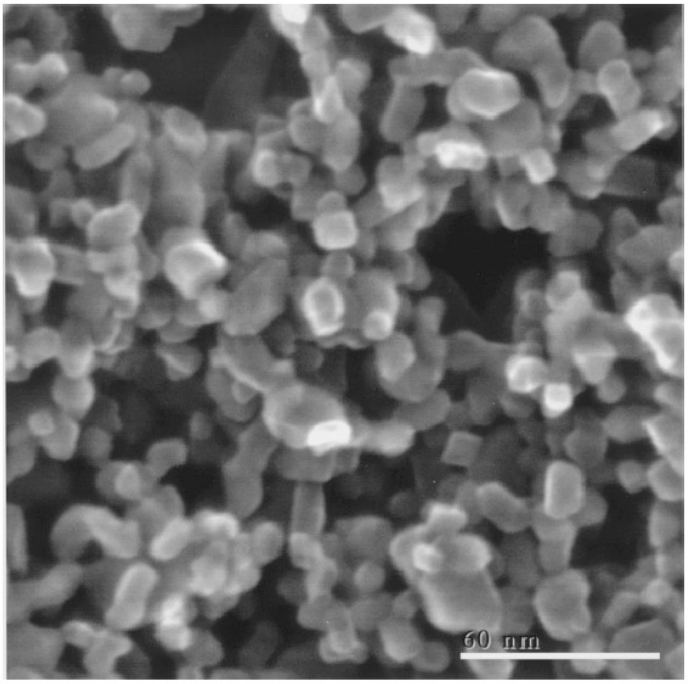

Figure 3 Scanning electron microscope picture of a nanocrystalline TiO_2 (anatase) film used in the dye-sensitized solar cell (DYSC)

*Taken from the Fig. 2 of Ref. 8

DYSC Performance

The high contact area of the junction nanocrystalline solar cells renders the understanding and control of interfacial effects essential for future improvement of cell performance. It is important to determine the nature of the exposed surface planes of the oxide and the mode of interaction with the dye. For the adsorption of the N3 dye on TiO_2 this is now quite well understood. The prevalent orientation of the anatase surface planes is (101) and the sensitizer if adsorbed through two of the four carboxylate groups, at least one of them being anchored via a bidentate configuration bridging two adjacent titanium sites [16].

At this stage the confirmed efficiency obtained with the black dye is 10.4% as shown in Fig. 4 [17]. Further development will concentrate on the enhancement of the photoresponse in the near IR region. The goal is to obtain a DYSC having optical features similar to GaAs. A nearly vertical rise of the photocurrent close to the 920 nm absorption threshold would increase the short circuit photocurrent from currently 20.5 to about 28 mA/cm^2. With the V_{oc} and FF values of Fig. 4, this would raise the overall efficiency to 14.2%.

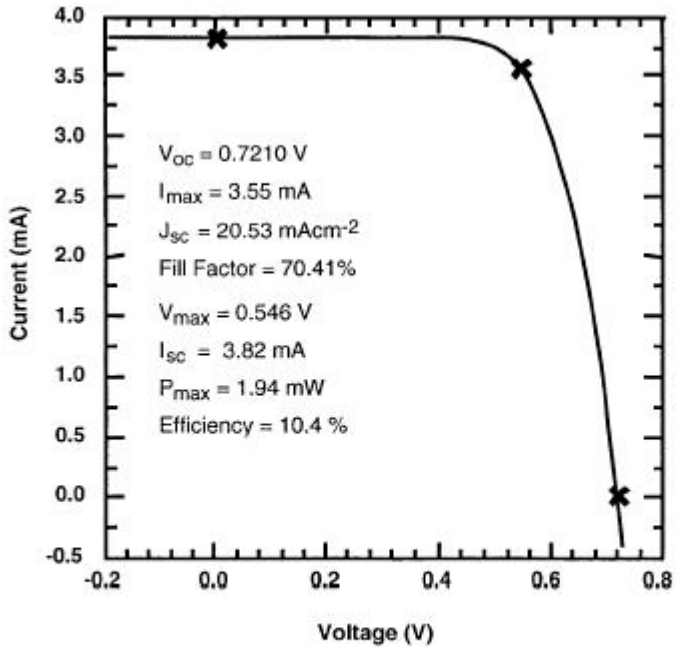

Fig. 4 Photocurrent-voltage characteristic of a nanocrystalling solar cell sensitized with the black day. The results shown were obtained at the NREL calibration Laboratory. A light source simulating AM 1.5 globe radiation was used, with 100 mW/cm2 incident intensity.

*Taken from the Fig. 4 of Ref. 17

An advantage of the DYSC is that its performance is remarkably insensitive to temperature change. Thus, raising the temperature from 20 to 60 ºC has no effect on the power conversion efficiency. Stability studies have shown the DYSC sustain temperatures of 85 ºC without loss of performance.

Conclusion

An important standard of living will require an abundant, inexpensive and decentralized energy source, solar energy seems ideally suited for this application. The dye-sensitized solar cell is at present the only serious competitor to solid state junction devices for the conversion of solar energy into electricity. Recent developments in the area of sensitizers for these devices have led to dyes which absorb across the visible spectrum leading to higher efficiencies and hold great potential for further cost reduction and simplification of the manufacturing of dye solar cells.

Reference:

[1] Nelson, J. The Physics of Solar cells. ISBN 1-86094-340-3; Imperial College Press: London, U.K., **2003**.

[2] West , W.; Proceedings of Vogel Centennial Symposium, Photogr. Sci. Eng. **1974**, 18, 35 .

[3] Moser , J. Monatsch. Chem. **1987**, 8, 373.

[4] Namba , S.; Hishiki , Y. J. Phys. Chem. **1965**, 69, 774.

[5] Gerischer , H.; Tributsch , H. Ber. Bunsenges. Phys. Chem. **1968**, 72, 437.

[6] O'Regan , B.; Graẗze, M. Nature. **1991**, 252, 737.

[7] Graẗze, M. Nature (London). **2000**, 403, 363.

[8] Graẗze, M; Prog. Photovolt. Res. Appl. **2000**,8,171.

[9] Amadelli, R.; Argazzi, R.; Bignozzi, C. A.; Scandola, F. J. Am. Chem. Soc., **1990**, 112, 7029 .

[10] Nazeeruddin, M. K.; Kay, A.; Rodicio, I.; Humphrey-Baker, R.; MuE ller, E. ; Liska, P.; Vlachopoulos, N.; Graẗze, M. J. Am. Chem. Soc. **1993**, 115, 6382.

[11] Tachibana, Y.; Moser, J. E.; Graẗze, M,; Klug , D. R.; Durrant, J. R. J. Phys. Chem. **1996**, 100, 20056.

[12] Ashbury, J. B.; Ellington, R. T.; Gosh, H. N.; Ferrere, S.; Nozik, A. J.; Lian, T.; J. Phys. Chem. B. **1999**, 103, 3110.

[13] Nazeeruddin, M. K.; Pechy , P.; Graẗze, M, Chem. Commun. **1997**, 85, 1075.

[14] Polo, A.S. Coordination Chemistry Reviews **2004**, 248, 1343.

[15] Barbe, C. J.; Arendse, F.; Comte, P.; Jirousek, M.; Lenzmann, F.; Shklver , V.; Graẗze, M. J. Am. Chem. Soc. **1997**, 80, 3157.

[16] Shklover, V.; Ovchinnikov ,Yu. E.; Braginsky, L. S.; Zakeeruddin , S. M.; Graẗze, M. Chem. Mater. **1998**, 10, 2533.

[17] Haggeldt , A.; Graẗze, M. Acc. Chem. Res. **2000**,33, 269.